

Magnetism and high-magnetic field magnetization in alkali superoxide CsO_2

Mizuki Miyajima^{1*}, Fahmi Astuti^{2,3}, Takeshi Kakuto¹, Akira Matsuo⁴, Dita P. Sari^{2,5}, Retno Asih^{2,5}, Kouichi Okunishi⁶, Takehito Nakano⁵, Yasuo Nozue⁵, Koichi Kindo⁴, Isao Watanabe^{2,3,5} and Takashi Kambe^{1†}

¹Department of Physics, Okayama University, Okayama 700-8530, Japan

² Advanced Meson Science Laboratory, RIKEN Nishina Center, Wako, Saitama 351-0198, Japan

³ Department of Physics, Hokkaido University, Sapporo 060-0808, Japan

⁴ Institute for Solid State Physics, The University of Tokyo, Kashiwa, Chiba 277-8581, Japan

⁵ Department of Physics, Osaka University, Toyonaka, Osaka 560-0043, Japan

⁶ Department of Physics, Niigata University, Niigata 950-2181, Japan

*p2qm1zzv@s.okayama-u.ac.jp

†kambe@science.okayama-u.ac.jp

Abstract

Alkali superoxide CsO_2 is one of candidates for the spin- $\frac{1}{2}$ one-dimensional (1D) antiferromagnet, which may be sequentially caused by an ordering of the π -orbital of O_2^- molecule below $T_S \sim 70$ K. Here, we report on the magnetism in powder CsO_2 and high-magnetic field magnetization measurements in pulsed-magnetic fields of up to 60 T. We obtained the low temperature phase diagram around the antiferromagnetic ordering temperature $T_N = 9.6$ K under the magnetic field. At 1.3 K, remarkable up-turn curvature in the magnetization around a saturation field of ~ 60 T is found, indicating the low-dimensional nature of the spin system. The saturated magnetization is also estimated to be $\sim 1\mu_B$, which corresponds to the spin- $\frac{1}{2}$. We will compare it with the theoretical calculation.

O_2 is a magnetic molecule with a spin-1, originating with two unpaired electrons on antibonding π^* orbitals. The magnetism of three structural phases of solid O_2 has been studied long ago [1, 2]. The magnetic exchange interaction between O_2 molecules depends strongly on their distance as well as relative displacement [1, 2]. O_2 molecules adsorbed in a porous metal complexes have been investigated by a magnetic susceptibility and high magnetic field magnetization [3, 4]. The O_2 -array is confined in the nano-channel region and exhibits a metamagnetic transition under high-magnetic field, which is considered to be due to a configurational transition of O_2 dimer. Other candidate for O_2 molecular based magnet is achieved by a encapsulation of O_2 molecules in single-walled carbon nanotubes. From the magnetic susceptibility and high-magnetic field magnetization, it is proposed as a spin-1 Haldane state [5]. Since then, the magnetism of O_2 molecule has been attracted much attention.

Magnetism of alkali superoxide, AO_2 ($A = \text{Na}, \text{K}, \text{Rb}$ and Cs), originates in unpaired π -electron on the O_2^- molecular anion, where one electron transfers from the alkali metal to O_2 making a spin- $\frac{1}{2}$ state. The transferred electron has a freedom which orbital (π_x^* or π_y^*) to select and the orbital ordering would be expected to realize the three-dimensional magnetic exchange pathways. At room temperature, it is proposed that KO_2 , RbO_2 and CsO_2 have the same tetragonal crystal structure ($I4/mmm$) while NaO_2 has a cubic crystal structure ($\text{Fm}\bar{3}m$). Recently, CsO_2 has been attracted considerable attention because of the one-dimensional (1D) antiferromagnetic (AF) nature [6]. Below the structural phase transition temperature $T_S = 70$ K, the magnetic susceptibility follows a well-known Bonner-Fisher curve. It is proposed that the structural phase transition is accompanied

with the π -orbital ordering of O_2 molecules, which leads to a zig-zag like 1D chain along the b -axis. If this is the case, the 1D AF super-exchange pathway might be via the Cs atom. NMR experiment shown a power-law decay in inverse spin-lattice relaxation rate at low temperature, suggesting that the ground state of CsO_2 is a Tomonaga-Luttinger liquid (TLL) state [7]. At lower temperatures, it was proposed that CsO_2 showed an AF transition at $T_N = 9.6$ K [6, 8], but the low temperature magnetism of CsO_2 have not yet been clarified.

KO_2 and RbO_2 also showed AF transitions at $T_N = 7$ and 15 K, respectively [8]. In spite of the same crystal structures as CsO_2 at room temperature, their magnetic susceptibilities show Curie-Weiss behavior from room temperature to T_N , but do not show the 1D behaviors. As the low-temperature structures in KO_2 and RbO_2 have not been settled, the magnetic exchange pathway have not been determined yet. Moreover, in NaO_2 , both the low temperature structure and the magnetic ground state is still under debate. Therefore, clarifying how the structure changes at low temperature is important subject to understand the correlation between the orbital ordering and the magnetism.

Accordingly, alkali superoxide is one of the fascinating candidates for molecular based low-dimensional magnet and may have a strong coupling between spin and orbital degrees of freedom. In this Letter, we have shown the low-temperature magnetism of CsO_2 , especially, high-magnetic field magnetization for the first time. We will present the full temperature dependence of magnetization around T_N in order to discuss the magnetic phase diagram. To discuss the dimensionality of CsO_2 , the high-field magnetization will be compared with the theoretical calculation.

We synthesized CsO_2 powder using a liquid ammonia method. Alkali-metal was placed in a glass tube in a Ar-filled glove box (O_2 and $\text{H}_2\text{O} < 0.1$ ppm) that was then dynamically pumped down to 10^{-2} Pa. The glass tube was cooled by liquid N_2 in order to condense the NH_3 . After the glass tube was filled with liquid NH_3 (typically, ~ 10 ml), O_2 gas was put in at a constant pressure of ~ 0.1 MPa. The solution was kept at -40°C . The reaction can be recognized complete when the solution became colorless and the product precipitated. Then, we removed the liquid NH_3 by dynamically pumping the glass tube, and obtained CsO_2 powder. The color of CsO_2 powder is dark yellow. The X-ray powder diffraction (XRPD) patterns of the samples were measured with synchrotron radiation at BL-8A of KEK-PF (wave length $\lambda = 0.99917\text{\AA}$). Rietveld refinement was performed to obtain the structural parameters using the GSAS II package [9]. The final weighted R -factor, R_{wp} , for room temperature structure was converged to 4.36 %, indicating a good fit to the experimental data. The magnetization, M , was measured using a

SQUID magnetometer (MPMS-R2 and MPMS3, Quantum Design Co. Ltd.) in the temperature region > 2 K. High magnetic field magnetization was measured in pulsed magnetic fields up to 60 T below 1.3 K. Because the CsO_2 sample is very sensitive to the atmosphere, the samples must be handled in the Ar-filled glove box.

Figure 1 (a) shows the XRPD pattern of CsO_2 at room temperature. All peaks can be indexed by the tetragonal symmetry (I4/mmm). Very small amount of impurity was confirmed to be $\text{CsOH}\cdot\text{H}_2\text{O}$, which fraction was estimated to be less than 3 % from the XRPD analysis. This impurity phase should not influence the intrinsic magnetic property of CsO_2 because it has no unpaired electrons. The inset of figure 1 (a) depicts the schematic figure of the crystal structure for the room temperature phase of CsO_2 . The lattice parameter of CsO_2 is estimated to be $a = 4.469\text{\AA}$ and $c = 7.324\text{\AA}$, which is consistent with the literature [6]. The O–O distance is estimated to be 1.11\AA , which may be effectively reduced by the libration of O_2 molecule.

Figure 1 (b) shows the temperature dependence of inverse magnetic susceptibility, χ^{-1} , of CsO_2 under a field cooling condition. The applied magnetic field is 0.1 T. No Curie-tail at low temperatures indicates high-quality of this sample. In the paramagnetic region, from room temperature to $T_1 \sim 150$ K, the χ follows Curie-Weiss law with Weiss temperature, $\theta = -10.1$ K, and effective magnetic moment, $\mu_{\text{eff}} = 1.95\mu_B$ while from T_1 to $T_S \sim 70$ K, $\theta = -30.0$ K and $\mu_{\text{eff}} = 2.05\mu_B$, where μ_B is Bohr magneton. T_S corresponds to the reported structural phase transition temperature [6]. The μ_{eff} is slightly larger than the value expected from $\text{spin-}\frac{1}{2}$, suggesting the orbital contribution. These values of θ and μ_{eff} are consistent with the previous results [6, 10]. We note that the change in χ around T_1 can be recognized in a different sample batch. Accordingly, the AF interaction among the spins on O_2 molecules becomes more dominant below T_1 . In the inset of figure 1 (b), the (200) Bragg reflection in the high-temperature tetragonal phase splits into two peaks with (200) and (020) indices below 150 K, suggesting a tetragonal-to-orthorhombic structural change around 150 K. Thus, the structural phase transition at T_1 should be related with the enhancement of AF interactions. We will discuss the structural study in a separated paper in detail.

Below T_S , the χ shows a broad maximum around 28 K, indicating a low-dimensional character of the spin system. As shown in the figure 1 (c), the χ below T_S can be fitted by the well-known Bonner-Fisher formula [11]. When we write the antiferromagnetic Heisenberg Hamiltonian as $\mathcal{H} = -J_{1D} \sum_i \mathbf{S}_i \cdot \mathbf{S}_{i+1}$, the 1D AF interaction, J_{1D}/k_B , is estimated to be 42.8 K, where k_B is a Boltzmann

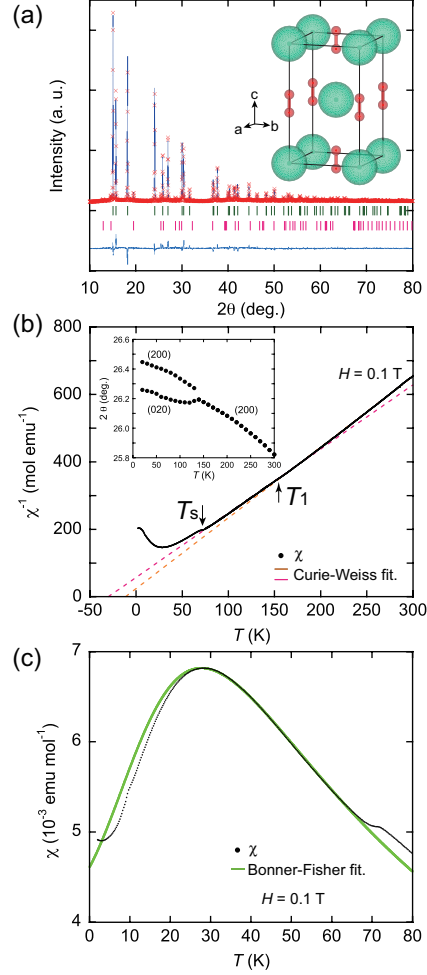


Figure 1: (a) Room temperature X-ray powder diffraction pattern collected from CsO_2 using $\lambda = 0.99917\text{\AA}$. Observed data (red crosses), the calculated pattern (blue line), the candidate peak positions (light green bar for CsO_2 and pink bar for $\text{CsOH}\cdot\text{H}_2\text{O}$) and the difference between the observed and the calculated data (light blue line) are shown. The inset depicts the room-temperature structure of CsO_2 , where Cs and O atoms are shown by the green and the red spheres, respectively. (b) Temperature dependence of inverse magnetic susceptibility, χ^{-1} , of CsO_2 (black dots) with Curie-Weiss fits (pink and orange dotted lines). The fitted parameters are described in the text. (c) Temperature dependence of χ (black dots) below T_S with a Bonner-Fisher fit (light green line). The anomaly at $T_N = 9.6$ K corresponds to the AF ordering.

constant. The obtained J_{1D}/k_B is consistent with the previous results [6, 7]. We could not observe the shift of temperature, at which the χ showed the maximum, under the magnetic field up to 7 T. The shift is evidenced in the TLL phase in the spin- $\frac{1}{2}$ AF $\text{Cu}(\text{C}_4\text{H}_4\text{N}_2)(\text{NO}_3)_2$ [12].

The anomaly at $T_N = 9.6$ K corresponds to the AF ordering [6]. Figure 2 (a) shows the temperature dependence of M/H at several magnetic fields. When the magnetic field was increased above 3 T, the M/H increased at low temperatures, suggesting the existence of a spin-flop transition around 3 T. Figure 2 (b) shows the isothermal derivative magnetization data, dM/dH , as a function of magnetic field around T_N . The anomalies around 3 T (arrows in the figure 2 (b)) are clearly observed and shifted higher fields side with increasing temperatures. In pulsed magnetization experiments, the magnetization curves also indicate the magnetic phase transition around 2.49 T. We summarize a possible phase diagram of CsO_2 under the magnetic field in the figure 2(c). This magnetic phase diagram is typical of the antiferromagnet with an easy-axis anisotropy, and the phase transition from the AF-1 to the AF-2 phase should correspond to the spin-flop transition. We note that no hysteresis in the magnetization curve was observed.

Figure 3 (a) shows the magnetization and its derivative curves for CsO_2 as a function of magnetic field up to 60 T at 1.3 K. Below T_N , remarkable up-turn curvature in the magnetization around a saturation field of ~ 60 T is found, suggesting the low-dimensional nature of this spin system. The saturated magnetization is also estimated to be $\sim 1\mu_B$, which corresponds to the spin- $\frac{1}{2}$. This is consistent with the magnetic susceptibility experiments. As shown in figure 3 (b), the fit with the Bethe-ansatz curve [13] gives the saturation magnetization of $H_S = 50$ T and $J_{1D}/k_B = 38.6$ K. From this, low-field magnetization can be reproduced by the exact curve, but, at high-field region, especially around H_S , the high-field magnetization seems to be inconsistent with the calculation. On the other hand, if we used the $J_{1D}/k_B = 42.8$ K estimated from the Bonner-Fisher fit in fig. 1 (c), the calculated magnetization did not reproduce the experiments as a whole. We may introduce a thermal effect and/or a higher-dimensionality of the spin system, i.e., an interchain coupling, to settle these inconsistency. The magnetization curve for temperature $T/J_{1D} = 0.1$ with $J_{1D}/k_B = 38.6$ K in fig. 3 (b), which was calculated by a finite temperature DMRG [14], implies better agreement around the saturation field, but could not reproduce the experiments entirely. Thus, the inconsistency around the saturation field in CsO_2 may be caused by the interchain couplings.

Using the molecular field approximation, we estimate the magnetic exchange interaction and the anisotropy in CsO_2 . The spin flop field, H_{SF} , can be written by

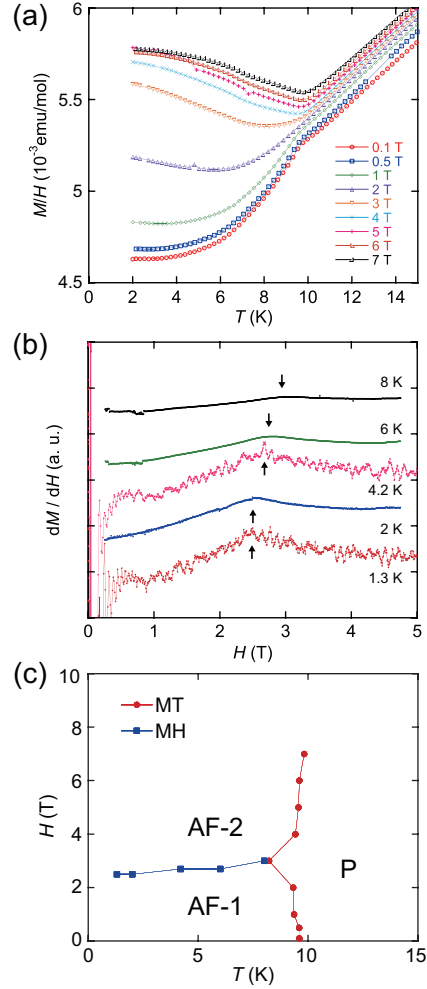


Figure 2: (a) Temperature dependence of M/H for CsO₂ at several magnetic fields. (b) Isothermal derivative magnetization data, dM/dH , as a function of magnetic field below T_N . The data at 1.3 K and 4.2 K were obtained by the pulsed magnetic field experiments while the others were obtained by differentiating the MPMS data. The arrows point at anomaly in the dM/dH plot for different temperatures, indicating the spin-flop transition fields. The data are shifted for clarity. (c) A possible phase diagram of CsO₂, where P, AF-1 and AF-2 represent a paramagnetic, an antiferromagnetic-1 and an antiferromagnetic-2 phase, respectively. The red circles are obtained from the temperature dependence of magnetization (MT) while the blue squares are obtained from the magnetic field dependence of magnetization (MH).

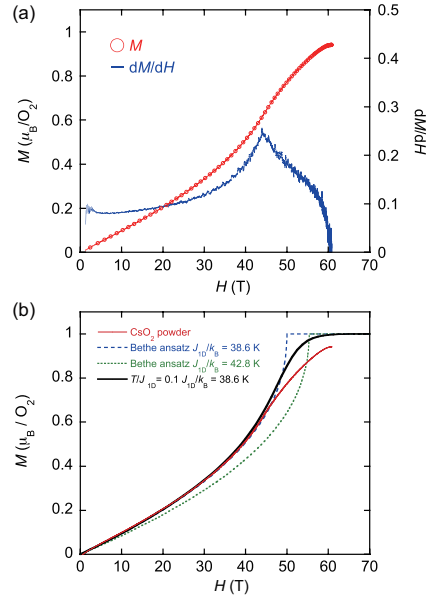


Figure 3: (a) High magnetic field magnetization, M , curve (red circles) and its derivative, dM/dH , curve (blue line) for CsO₂ at 1.3 K. In the vertical axis, $M = 1$ corresponds to $1\mu_B$ per the O₂ molecule, indicating the spin- $\frac{1}{2}$. (b) The dashed lines are Bethe-ansatz results for $T = 0$ with $J_{1D}/k_B = 38.6$ K (blue dashed line) and $J_{1D}/k_B = 42.8$ K (green dashed line). The black line shows the theoretical calculation with $T/J_{1D} = 0.1$ and $J_{1D}/k_B = 38.6$ K.

the exchange field, H_E , and the anisotropy field, H_A , as follows;

$$H_{SF} = \sqrt{2H_E H_A} \quad (1)$$

The H_E can be written as $H_E = zJS/g\mu_B$, where z is a number of nearest neighbor spins. If we assume $z = 2$ for the orbital ordered structure of CsO_2 , which should corresponds to a 1D spin chain, the magnetic exchange interaction $J_{1D}/k_B = 38.6$ K gives the H_E of 250 kOe. From the figure 2, the H_{SF} is estimated to be 2.49 Tesla at 2 K. Using these values, H_A is obtained to be 1.24 kOe. The H_A is almost comparable to the dipolar anisotropy field calculated in α -phase of solid O_2 [2].

Knaflitz *et al.* found a disappearance of electron paramagnetic resonance (EPR) signals in the vicinity of T_N and observed an antiferromagnetic resonance (AFMR) around zero-magnetic field below T_N using X-band frequency [15]. We also observed the disappearance of EPR signals in the vicinity of T_N , implying a bulk long-range magnetic ordering. The muon spin relaxation experiments (μSR) also show clear muon-spin precession even in the zero-field condition below T_N , [16] proving that the ground state of CsO_2 under the magnetic field is not a field-induced ordered state, which claimed by the authors [15]. Although we tried to measure the AFMR using the X-band frequency, no corresponding AFMR signal were found down to 5 K. The AFMR relation strongly depends on the anisotropy as well as the magnetic field. We speculate that our measured frequency is too high compared with the zero-field excitation energy to observe the AFMR signal. On the contrary, the observed AFMR field may not be simply explained by a general AFMR relation with an uniaxial anisotropy. As the EPR field at X-band frequency is about 0.3 T, which is one-order of magnitude smaller than the H_{SF} , the AFMR signal at the X-band frequency may be observed at a magnetic field around the H_{SF} , which is higher than the observed field, if we assume only the uniaxial anisotropy. Therefore, other anisotropy may be taken into consideration to explain the observation of AFMR around zero magnetic field at the X-band frequency. In fact, in the α -phase of solid O_2 , orthorhombic magnetic anisotropy was estimated from the AFMR, where it is suggested that the one is originated from the O_2 molecule itself and the other from the dipolar interaction [2].

The magnetic exchange interactions have been calculated in the orbital-ordered KO_2 , in which both the crystal field from the cations and the Coulomb interactions are thought to be dominant [17, 18]. Kim *et al.* suggested that the coherent ferro-orbital ordering of O_2 molecules was important to realize the experimentally observed AF structure [19]. In CsO_2 , it is proposed from the XRPD and the Raman scattering experiments that the low temperature structure has a $a \times 2b \times 2c$

periodicity, which may be accompanied with the coherent tilting of O_2 molecular axis [6]. This would lead to ferro-orbital ordering of O_2 molecules along the [100] direction and antiferro-orbital ordering along the [010] and [111] directions. If we consider the magnetic super-exchange interaction via Cs^+ ions between the nearest neighbor (NN) O_2 molecules with the framework of the Kanamori-Goodenough rule [20], it may be expected that the ferro-magnetic interaction is dominant along the [100] direction while the antiferromagnetic interaction along the [010] and [111] directions. The [010] direction had been proposed as the 1D axis. If we refer the calculated exchange interaction in KO_2 , the interchain magnetic exchange interactions between NN O_2 molecules may be enough to induce the long-range magnetic ordering in CsO_2 . On the contrary, it has already been mentioned that CsO_2 shows another structural phase change around $T_1 = 150$ K. Thus, to understand the magnetic exchange interaction between O_2 molecules, the exact orbital-ordered structure at low temperature should be indispensable.

In conclusion, we have synthesized high-quality CsO_2 and investigated the magnetic properties. The obtained magnetic phase diagram is similar to that for the antiferromagnet with an easy axis anisotropy. High magnetic field magnetization of CsO_2 was performed up to 60 Tesla for the first time and exhibited remarkable up-turn curvature around the saturation field, implying that CsO_2 is a candidate for quasi-1D spin- $\frac{1}{2}$ antiferromagnet. On the other hand, the theoretical calculation with $T = 0$ and $T/J_{1D} = 0.1$ could not wholly reproduce the experiment. To settle these inconsistency, further experiments including the low-temperature structure should be highly desirable.

We would like to thank Prof. T. C. Kobayashi for valuable discussions on magnetism of CsO_2 . The X-ray diffraction patterns were measured in research projects (2017G636) of KEK-PF. This research is partly supported by KAKENHI grants from Japan Society for the Promotion of Science (15H03529).

References

- [1] M. C. van Hemert, et al., Phys. Rev. Lett., 51, 1167 (1983).
- [2] C. Uyeda, K. Sugiyama and M. Date, J. Phys. Soc. Jpn., 54, 1107, (1985). and references therein.
- [3] T. C. Kobayashi, et al., Prog. Theor. Phys. Suppl., 159, 271 (2005).
- [4] A. Hori, et al., J. Phys. Soc. Jpn., 82, 084703, (2013).

- [5] M. Hagiwara, et al., J. Phys. Soc. Jpn., 83, 113706, (2014).
- [6] S. Riyadi, et al., Phys. Rev. Lett., 108, 217206 (2012).
- [7] M. Klanjšek, et al., Phys. Rev. Lett., 115, 057205 (2015).
- [8] W. Hesse, et al., Prog. Solid State Chem. 19, 47 (1989).
- [9] Toby, B. H., Von Dreele, R. B., J. Appl. Cryst., 46(2), 544-549 (2013).
- [10] A. Zumsteg, et al., Phys. Cond. Matter 17, 267-291 (1974).
- [11] J. C. Bonner and M. E. Fisher, Phys. Rev., 135, A640 (1964). W. E. Estes et al., Inorg, Chem., 17, 1415 (1978).
- [12] Y. Kono, et al., Phys. Rev. Lett. 114, 037202 (2015).
- [13] R. B. Griffiths, Phys. Rev., 133, A768 (1964).
- [14] K. Okunishi, Phys. Rev. B 60, 4043 (1999).
- [15] T. Knafllic, et al., Phys. Rev. B., 91, 174419 (2015).
- [16] F. Astuti, M. Miyajima, D. P. Sari, R. Asih, T. Nakano, Y. Nozue, T. Kakuto, T. Kambe, I. Watanabe, in preparation.
- [17] M. Kim, et al., Phys. Rev. B., 81, 100409(R) (2010).
- [18] I. V. Solovyev, New J. of Phys., 10, 013035 (2008)., I. V. Solovyev, Z. V. Pchelkina and V. V. Mazurenko, Crys. Eng. Comm., 16, 522 (2014).
- [19] H. G. Smith, et al., J. Appl. Phys. 37, 1047 (1966).
- [20] J. B. Goodenough, Magnetism and the Chemical Bond (Interscience Publishers, New York, 1976)., J. Kanamori, J. Phys. Chem. Solids 10, 87 (1959).